Talanta 84 (2011) 572–578

Contents lists available at ScienceDirect

Talanta

journal homepage: www.elsevier.com/locate/talanta

Depth profile characterization of Zn–TiO_2 nanocomposite films by pulsed radiofrequency glow discharge-optical emission spectrometry

Deborah Alberts[a], Beatriz Fernández[a,*], Tania Frade[b], Anabela Gomes[b], Maria Isabel da Silva Pereira[b], Rosario Pereiro[a], Alfredo Sanz-Medel[a,*]

[a] University of Oviedo, Department of Physical and Analytical Chemistry, Julian Claveria, 8, 33006 Oviedo, Spain
[b] CCMM, Department of Chemistry and Biochemistry, University of Lisbon, Campo Grande C8, 1749-016 Lisbon, Portugal

ARTICLE INFO

Article history:
Received 1 December 2010
Received in revised form 18 January 2011
Accepted 30 January 2011
Available online 4 February 2011

Keywords:
Metal-matrix composites
Nanocomposites
Depth profiling analysis
Glow discharge optical emission spectrometry

ABSTRACT

In recent years particular effort is being devoted towards the development of radiofrequency (rf) pulsed glow discharges (GDs) coupled to optical emission spectrometry (OES) for depth profile analysis of materials with technological interest. In this work, pulsed rf-GD-OES is investigated for the fast and sensitive depth characterization of Zn–TiO_2 nanocomposite films deposited on conductive substrates (Ti and steel). The first part of this work focuses on assessing the advantages of pulsed GDs, in comparison with the continuous GD, in terms of analytical emission intensities and emission yields. Next, the capability of pulsed rf-GD-OES for determination of thickness and compositional depth profiles is demonstrated by resorting to a simple multi-matrix calibration procedure. A rf forward power of 75 W, a pressure of 600 Pa, 10 kHz pulse frequency and 50% duty cycle were selected as GD operation parameters.Quantitative depth profiles obtained with the GD proposed methodology for Zn–TiO_2 nanocomposite films, prepared by the occlusion electrodeposition method using pulsed reverse current electrolysis, have proved to be in good agreement with results achieved by complementary techniques, including scanning electron microscopy and inductively coupled plasma-mass spectrometry. The work carried out demonstrates that pulsed rf-GD-OES is a promising tool for the fast analytical characterization of nanocomposite films.

1. Introduction

Research at the nanometer scale, aiming at creating novel materials and devices offering better performance than those of macro/micro systems, is currently of great relevance in many branches of modern science, technology and engineering [1]. In coatings technology, the introduction of nanocomposite films, offering excellent properties in different applications [2–4], represents a real analytical challenge for their fast and reliable morphological, structural and depth profiling characterization.

Electrodeposition techniques provide an excellent route for the synthesis of nanocomposite coatings with metallic matrices, where a wide variety of spherical shaped nanosized particles can be occluded, including SiO_2 [5], TiO_2 [6] and Al_2O_3 [7]. Zn has been widely used as the base of different surface coatings for ferrous materials. Compared to Zn plating, Zn based composites exhibit better corrosion protection and enhanced mechanical properties [8,9]. On the other hand, TiO_2 nanosized particles are of great interest due to their increasing availability, low cost, high chemical stability and their almost ideal photocatalyst behavior. Thus, they are currently excellent candidates for environmental purification processes, particularly in the treatment of polluted water [10] and so, the interest on Zn–TiO_2 nanocomposite films is steadily growing.

Depth profile analysis spectrometric techniques [1] offer great potential for the characterization of nanocomposite films because they provide information on major and trace constituents to better understand the processes occurring at nanometer length dimensions (e.g. distribution and concentration of nanosized particles through the layer, possible diffusion processes, presence of impurities, etc.) having a direct influence on the final properties of the coatings. Glow discharges (GD) have been widely investigated as powerful atomization, excitation and ionization tools, both for optical emission (OES) and for mass spectrometry (MS) detection and their capability to generate atoms and ions directly from the solid samples, following an atomic "layer-by-layer" approach [11] is well known. The application of GD analytical techniques for depth profiling analysis is continuously growing because they offer interesting advantages, including high depth resolution (<5 nm)

* Corresponding authors at: Department of Physical and Analytical Chemistry, Faculty of Chemistry, University of Oviedo, Julian Clavería 8, 33006 Oviedo, Spain. Tel.: +34 985 10 34 74; fax: +34 985 10 34 74.
E-mail addresses: fernandezbeatriz@uniovi.es (B. Fernández), asm@uniovi.es (A. Sanz-Medel).

0039-9140/$ – see front matter © 2011 Elsevier B.V. All rights reserved.
doi:10.1016/j.talanta.2011.01.076

[12], fast sputtering rate, multielemental capability, low limits of detection (μg/g–ng/g) [13] and easiness of use. The advantageous features of GDs for depth profiling analysis arise from the nature of the sputtering mechanism, in which solid samples are stably and reproducibly sputtered with Ar ions of very low energy (<50 eV). Although GDs sources can offer depth profiling analysis with an excellent depth resolution, one of the major limitations of this technique is the limited lateral resolution, which is directly related to the size of the sampling orifice (in the order of 1–8 mm).

GDs operated in pulsed mode have been in the last decade proposed as attractive analytical alternatives to the more common continuous GD operation mode, because the pulsed mode allows high instantaneous power without inducing thermal degradation of the sample, as well as higher sensitivity and better depth resolution [14–16]. Moreover, different discharge processes take place at different times within a single pulse enabling (using an appropriate time-resolved signal acquisition detector) different types of analytical information along the pulse [17,18]. Important aspects related to pulsed GDs have been recently reviewed by Belenguer et al. [19].

The application of such pulsed GDs to Zn–TiO_2 nanocomposite films is investigated here. The nanocomposites are prepared by the occlusion electrodeposition method [20], and two different substrates were assayed: titanium and steel. The final properties of these nanocomposites will depend directly on their chemical composition and distribution and, therefore, the use of reliable depth profiling characterization techniques is of critical importance to assist the optimization of the synthesis procedures as well as to control the quality of the final coating. Analytical performance characteristics of radiofrequency (rf) pulsed GD-OES are investigated for such Zn–TiO_2 nanocomposite films and quantitative results are compared with those obtained by inductively coupled plasma (ICP) coupled to MS and by scanning electron microscopy (SEM) in order to assess the capability of GD sources for TiO_2 nanoparticles concentration and Zn–TiO_2 layer thickness determinations.

2. Materials and methods

2.1. Synthesis of Zn–TiO_2 nanocomposite coatings

Zn–TiO_2 nanocomposite films were obtained using pulsed reverse current electrolysis, from acidic zinc sulphate solutions, on a Ti and a steel support. The electroplating bath was a mixture of 0.60 mol dm^{-3} $ZnSO_4{\cdot}7H_2O$, 0.10 mol dm^{-3} $(NH_4)_2SO_4$ and 0.15 mol dm^{-3} H_3BO_3. For the preparation of the composites films 10 g dm^{-3} TiO_2 (Degussa P25) were added to the solution. The bath pH was adjusted to 4 by adding a H_2SO_4 diluted solution. The solutions were made daily without further purification, followed by de-aeration with nitrogen before and during the electrodeposition. A glass cell with two compartments was used, with a Zn plate as counter electrode and a commercial Ag/AgCl as reference (MeterLab, Radiometer). Two different substrates were employed for deposition of Zn–TiO_2 nanocomposite films; Ti (Goodfellow, Ti000430) and steel (Goodfellow, AISI 316L). The substrates were polished with 0.05-μm silica powder (Buehler) and ultrasonically cleaned for 10 min in pure water (resistivity 18 MΩ).

The values of the pulse-plating parameters employed in the preparation of Zn–TiO_2 were the following: 100 mA cm^{-2} for cathodic and anodic density pulse currents; 4 ms and 40 ms for on and off pulse durations, respectively; 9 mA for the average current and 9% of duty cycle at 23 Hz of cycle frequency. The deposition was performed under magnetic stirring (150 rpm) at room temperature during 100 min. After plating, the electrode was removed from the cell, rinsed with Millipore Milli-Q ultra pure water and dried under nitrogen atmosphere during 5–10 min at room temperature. Further details of the nanocomposite films preparation are described elsewhere [21]. Fig. 1a and b shows the morphology of the Zn–TiO_2 surface films, electrodeposited on a titanium and steel substrate, respectively. The SEM images reveal a rougher surface for the coatings deposited on steel substrate. The morphology of the metallic matrix depends on the substrate nature as well as the presence of TiO_2 nanoparticles in the coating.

Table 1
Emission lines selected.

Element	Wavelength (nm)	Element	Wavelength (nm)
O	130.21	S	361.47
C	156.14	Ti	365.35
Mn	258.43	Fe	371.99
Zn	335.50	Mo	379.82
Ni	341.47	Cr	425.43

2.2. Instrumentation for chemical analysis, morphological characterization and depth profiling analysis

ICP-MS was used to determine the total amount of Ti occluded in the coatings. Zn–TiO_2 nanocomposite films were analyzed after the deposition procedure by selective dissolution of the coating with HCl and H_2SO_4 aq. solutions. The sample preparation procedure followed for ICP-MS measurements was described by Deguchi et al. [22]. However, in order to dissolve the Zn–TiO_2 film without affecting the Ti substrate both the volume of acid solutions and the treatment time were lower than those used for the analysis of coatings deposited on steel substrates [20]. The instrument used was an Agilent 7500 (Agilent Technologies, Tokyo, Japan) equipped with a collision cell system.

The morphology, thickness and elemental composition (semi-quantitative analysis) of the coatings were investigated by SEM coupled with energy dispersive spectroscopy (EDS). SEM/EDS analyses were performed with a Quanta 400 instrument (FEI Company, Oregon, USA) coupled to an EDS analyzer (Oxford Instruments, UK). The electron beam voltage used was 20 kV.

Concerning depth profiling analysis, a rf-GD-OES instrument (Model JY 5000 RF) from Jobin Yvon Emission Horiba Group (Longjumeau Cedex, France) was used. The instrument is equipped with a standard GD source with an anode of 4 mm internal diameter and with two optical spectrometers (poly- and monochromator). One of the spectrometers is a 0.5 m Paschen Runge polychromator with a concave grating of 2400 lines mm^{-1} (110–800 nm of wavelength range) and the optical path purged with nitrogen. Also, the system is equipped with a Czerny-Turner monochromator (0.64 m focal length, blazed planar holographic grating of 2400 lines mm^{-1}), which allows the expansion of the instrument's capabilities to any wavelength of the spectral range (200–800 nm). Further details of the GD-OES instrument are described elsewhere [23].

Table 1 collects the wavelengths of the emission lines monitored for the elements of interest. The voltage applied to the photomultiplier tubes (PMT) was optimized for each wavelength to obtain maximum sensitivity and to avoid intensity saturation. PMT voltages were fixed at 550 V for Cr, 600 V for Ni, 650 V for Mo (measured in the monochromator), 700 V for Zn, C, Ti, and Fe and at 900 V for the other elements. In this work, net analytical signals were always considered (i.e. background subtracted). The samples were refrigerated at 0 °C by a cold liquid circulating between the sample and the rf power input. High-purity argon (99.999% minimum purity) from Air Liquide (Oviedo, Spain) was employed as discharge gas.

The operational mode 'constant pressure–constant forward power' was used throughout the experiments, for continuous and pulsed operation modes [24]. The reflected power was also monitored and kept always as low as possible (<1 W). Working in pulsed

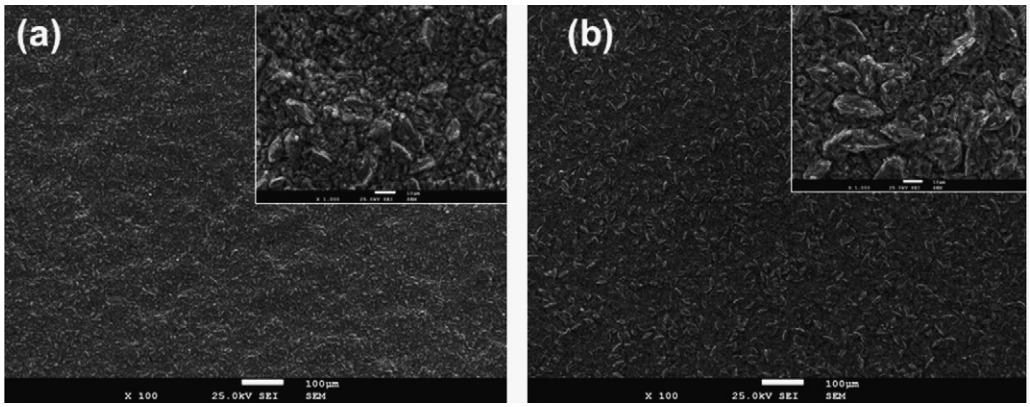

Fig. 1. SEM images of Zn–TiO_2 surface films, electrodeposited on (a) titanium and (b) steel substrates.

GD mode, apart from the Ar discharge pressure and rf forward power, three additional parameters have to be controlled and optimized: the pulse frequency, the pulse width, and the duty cycle [19]. Throughout the text, pulse frequency is understood as pulse repetition frequency, the pulse width is the duration of the power-on time for a single pulse, and the duty cycle is the ratio between the pulse-width and the sum of power-on and power-off time. After optimization, discharge conditions were fixed at 600 Pa for the Ar pressure and at 75 W for the rf forward power, pulse frequency was kept constant at 10 kHz and the duty cycle was fixed at 50%.

A multi-matrix calibration was performed for the quantification of rf-GD-OES profiles using a wide variety of bulk certified reference materials (CRMs). Multiple matrices (Fe, Ti, Ni, Al, Zn and Cu) as well as wide ranges of analyte mass fractions were used in the calibration curves: elemental concentrations varied from few μg/g up to high percentages (e.g. 99.6% Fe, 99.5% Ti, 97.5% Zn and 99.1% Ni). Before the analysis by rf-GD-OES, CRMs were polished using metallographic grinding papers (SiC: 220, 800 and 1200 grit) until obtaining a mirror-like surface and afterwards cleaned with ethanol to avoid contamination traces. The shape and depth of the craters were measured using a mechanical profilometer (Perth-ometer S5P, Mahr Perten, Germany). Two profile traces in different directions across the centre of each crater were measured in all cases. Sputtering rates, evaluated as mass loss per unit time during the sputtering, were calculated by measuring the penetration depths per unit time and considering the crater diameter and material density. The mean of three sputtered replicates was always used.

3. Results and discussion

3.1. Optimization of rf-GD operating conditions

The analyte emission intensity in GD-OES depends upon two main factors: the sputtering rate (determining the final density of analyte atoms in the plasma) and the excitation efficiency of these atoms (emission yield) [25]. Previous work carried out in our laboratory [26] demonstrated that enhanced emission intensities and emission yields (calculated as the ratio of the measured emission intensity and the sputtering rate) can be obtained in pulsed power mode by applying high pulse frequency and small duty cycles, in comparison with those obtained in the GD continuous mode counterpart. Moreover, it was found that less thermal-related problems and good crater shapes are obtained using such pulse conditions. Taking into account such results previously obtained, a detailed optimization of Ar discharge pressure and rf forward power using high pulse frequency and small duty cycles was performed to obtain a good crater shape and, therefore, to ensure a good depth resolution. Experimental parameters finally selected for all the subsequent measurements were: 600 Pa for the Ar discharge pressure, 75 W of rf forward power, 10 kHz of pulse frequency and 50% duty cycle (which means the average power is 37.5 W).

High quality GD analysis of coated samples mostly depends on the depth resolution and, therefore, on the experimental conditions selected for the analysis [27]. As it is well known, the crater bottom must be flat and with the crater walls perpendicular to the sample surface. Fig. 2 shows the crater shapes obtained for a Zn–TiO_2 nanocomposite film deposited on a steel substrate by pulsed rf-GD-OES, both at the coating/steel interface region (Fig. 2a) and at the steel substrate (Fig. 2b). To better appreciate the differences between the crater shapes, the profilometer scale has been selected individually and the crater depth is noted in each figure. As can be observed, crater shapes with perpendicular walls and rather flat crater bottom were obtained in both cases, indicating that the depth resolution in the rf-GD-OES profiles should be also good. Similar results were obtained for the Zn–TiO_2 nanocomposite films deposited on Ti substrates (Fig. 2c).

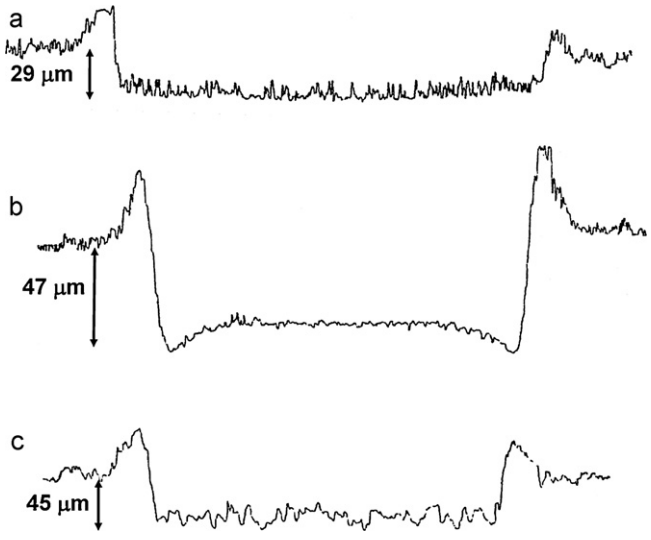

Fig. 2. Crater profiles obtained for a Zn–TiO_2 nanocomposite film deposited on steel and Ti substrates by pulsed rf-GD-OES at the optimized experimental conditions (600 Pa, 75 W, 10 kHz, 50% duty cycle): (a) at the coating/steel interface; (b) at the steel substrate; (c) at the Ti substrate.

3.2. Comparison of continuous and pulsed rf-GD-OES operation modes

One of the potential advantages of pulsed rf-GD sources arises from the creation of certain time regimes in which the background signal may be virtually suppressed while the analyte signal is enhanced. In recent previous work [28] we found that the intensity observed in the *prepeak* regime of the pulse can be 10 times larger than that of the plateau regime for resonance Cu lines and up to 5 times higher in case of metastable transitions, suggesting that the observed *prepeak* intensity increases were linked to an absence of self-absorption. This effect could improve the sensitivity of analytical calibration curves which is really important, for example, to identify possible contaminations on the Zn–TiO_2 nanocomposite films. Therefore, to explore the advantages of pulsed rf-GD-OES for TiO_2 detection, a critical comparison of intensity signals, sputtering rates and emission yields obtained by continuous and pulsed rf-GD-OES was first carried out. It is important to note that the commercial GD-OES instruments do not allow gated detection and, so, averaged signals over the pulse period are obtained.

Table 2 summarizes the signal intensities, the penetration rates and the emission yield ratios obtained for the Ti and O emission lines investigated by rf-GD-OES in continuous and pulsed mode. Five certified reference materials were employed for the study, covering a wide range of concentrations for Ti (from 2% to 89%) and one concentration for O (32%). As can be observed in the table, the sputtering rates obtained in pulsed mode were always lower than those obtained in continuous mode and this is consistent with the lower power deposited into the plasma (please note that the average power in pulsed mode is 37.5 W while 75 W are used in continuous mode). Also, significant differences of the observed analyte emission intensities and emission yields were apparent between continuous and pulsed operation modes. In the case of Ti, a notorious enhancement of intensity signals was clearly observed in pulsed mode: a 1.5-fold factor improvement was observed in all cases, independently of the Ti concentration (in the range of 2–89%) and the matrix of the sample. Moreover, it has to be highlighted that the emission yield for the Ti line, was about 2.5 times higher in the pulsed mode than in the steady-state counterpart (see ratios at the right part of Table 2). Concerning the oxygen behavior, only a slight improvement was observed for the emission yield (probably due, at least partly, to the low intensity signals measured at the emission line investigated as oxygen intensities were one order of magnitude lower than those obtained for Ti). From the experiments above, it is clear that even under the selected pulsed operation conditions (lower average rf power and without any time-gated detection) higher emission yields were obtained by pulsed mode. These findings show the potential of pulsed rf-GD-OES for future analysis of nanocomposite films.

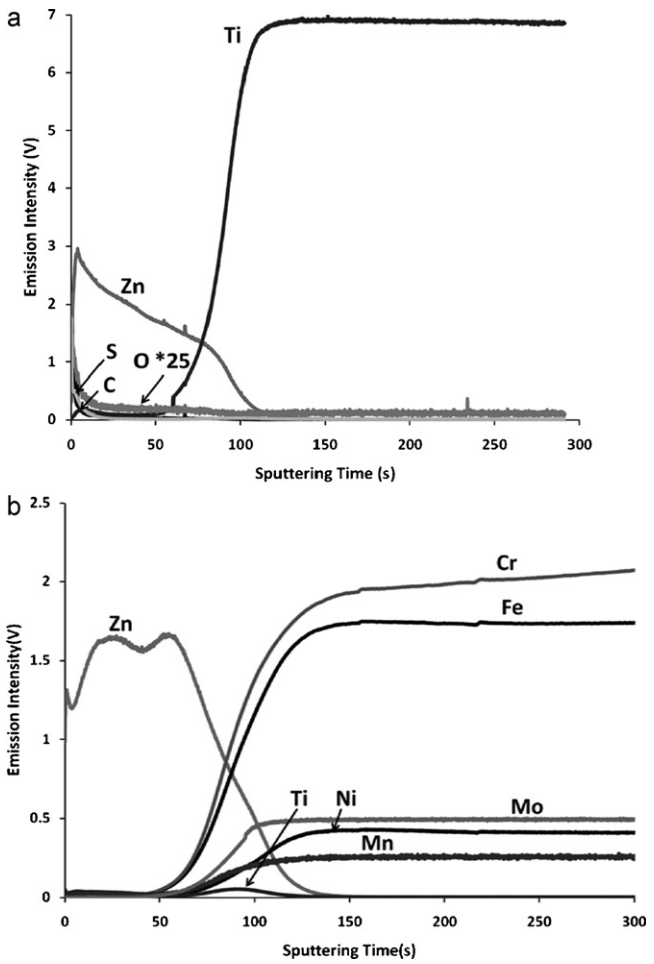

Fig. 3. Qualitative depth profiles obtained by pulsed rf-GD-OES for Zn–TiO_2 nanocomposite films at the optimized experimental conditions (600 Pa, 75 W, 10 kHz, 50% duty cycle): (a) deposited on a Ti substrate and (b) on a steel substrate.

3.3. Depth profiling characterization of Zn–TiO_2 nanocomposite films by pulsed rf-GD-OES

As pulsed rf-GDs allow improved emission intensities and emission yields for the elements of interest (compared to continuous operation mode), pulsed rf-GD-OES has been investigated in detail for depth profile characterization of Zn–TiO_2 nanocomposite films. Fig. 3a and b shows the qualitative depth profiles (ion signal intensities *versus* sample sputtering time) obtained by pulsed rf-GD-OES for the nanocomposite films deposited on a Ti and steel substrate,

Table 2
Values obtained by rf-GD-OES in continuous (600 Pa, 75 W) and pulsed mode (600 Pa, 75 W, 10 kHz, 50%) for the Ti and O emission intensities, sputtering rates and emission yields in four CRMs. Standard deviation values are calculated from the mean of three independent measurements.

Element (conc.%)	CRM	Measurement conditions	Intensity (V)	Penetration rate ($\mu m\,s^{-1}$)	Intensity/Penetration rate	Emission yield ratio
Ti (2%)	WASP 2[a]	Continuous	0.19 ± 0.0095	0.142 ± 0.011	1.33	2.35
		Pulsed	0.29 ± 0.012	0.092 ± 0.0059	3.12	
Ti (22%)	CC650A[b]	Continuous	0.34 ± 0.013	0.057 ± 0.0045	5.92	2.58
		Pulsed	0.53 ± 0.026	0.035 ± 0.0028	15.27	
Ti (25%)	JK41-1N[a]	Continuous	0.72 ± 0.036	0.133 ± 0.011	5.43	2.68
		Pulsed	1.09 ± 0.044	0.075 ± 0.0067	14.58	
Ti (89%)	175B[b]	Continuous	1.41 ± 0.061	0.092 ± 0.0064	15.38	2.50
		Pulsed	2.16 ± 0.101	0.056 ± 0.0045	38.38	
O (32%)	CC650A[b]	Continuous	0.058 ± 0.0023	0.057 ± 0.0051	1.02	1.10
		Pulsed	0.039 ± 0.0017	0.035 ± 0.0024	1.12	

[a] MBH Analytical Ltd., UK.
[b] SWEREA-KIMAB, Sweden

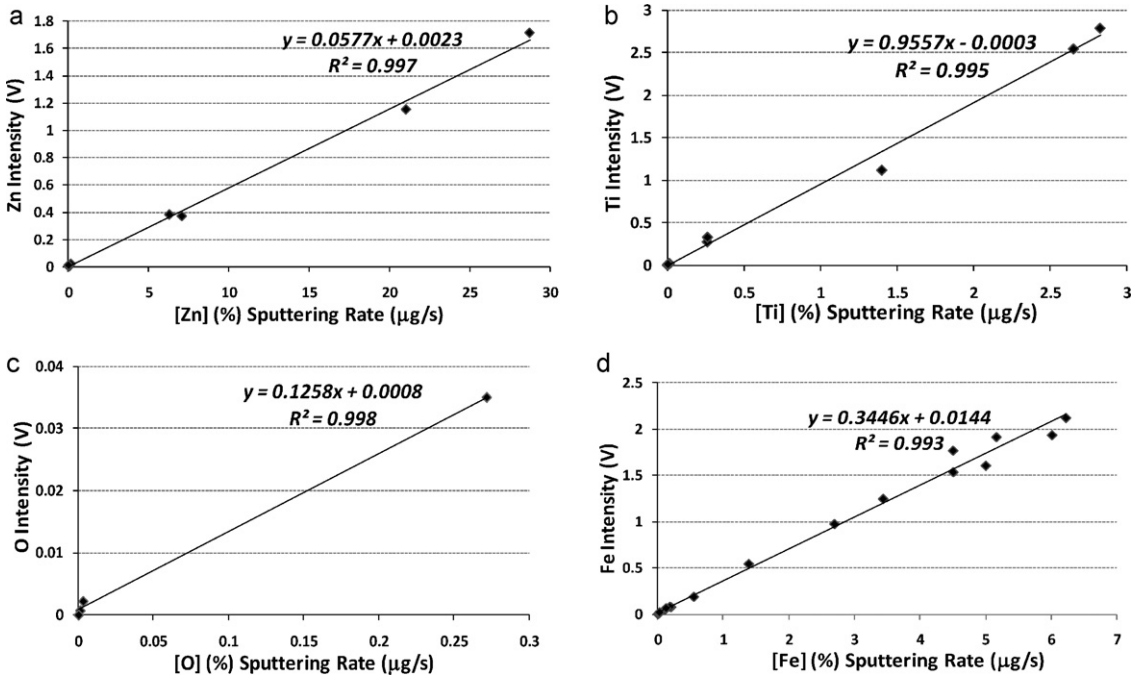

Fig. 4. Calibration curves obtained for (a) Zn, (b) Ti, (c) O and (d) Fe, by pulsed rf-GD-OES. Elemental concentrations are given in percentage and the sputtering rate in μg/s. Standard deviation values were calculated from the mean of three independent measurements, being in all cases in the range of 3–5%.

respectively. As can be observed, less than 100 s was needed in both cases to sputter the nanocomposite layer and reach the sample substrate. Furthermore, the Zn–TiO_2 film can be perfectly distinguished from the conductive substrates, following Zn and Ti profiles, with a good depth resolution. On the other hand, analysis of possible impurities in nanocomposite films is a critical aspect for the optimization of the sample preparation and electrodeposition processes and, therefore, quality control of impurities is mandatory for their subsequent applications. In Fig. 3a, a high intensity signal can be observed in the first seconds of analysis for O, C and S, indicating the contamination of the sample surface. These impurities could be attributed to the sample preparation procedure with different solutions (see section 2.1) and were also identified in the same nanocomposite films by semi-quantitative SEM/EDS analysis.

To convert the qualitative depth profiles obtained by pulsed GD-OES into quantitative depth profiles (mass content *versus* depth) a calibration graph must be constructed. Thus, calibration curves for all the elements present in the samples, both in the nanocomposite films and in the conductive substrates, were carried out. A multi-matrix calibration approach using homogeneous CRMs has been attempted here. Calibration graphs were obtained plotting the net intensity signals *versus* the product of the mass content of each element in the CRM and the sputtering rate of the standard (in $\mu g\, s^{-1}$). Fig. 4 shows four examples of the calibration plots obtained. As can be seen, the calibration curves obtained by pulsed rf-GD-OES for Zn, Ti, O and Fe showed a good linear relationship, with a high dynamic range.

The measured qualitative depth profiles (see Fig. 3a and b) were used to calculate the elemental concentrations, at each position of the depth profile, by making use of the calibration equations of Fig. 4. Fig. 5 shows the quantitative depth profiles obtained for the nanocomposite films under the selected operation conditions. In both cases, as can be seen, the interface between the Zn–TiO_2 layer and the substrate showed a good depth resolution with a sharp interface. Moreover, as can be seen in the enlarged profiles, at lower depths a homogeneous distribution of TiO_2 nanosized particles were found through the Zn layer in both cases, particularly for the TiO_2 nanoparticles deposited on to the steel substrate (see Fig. 5b).

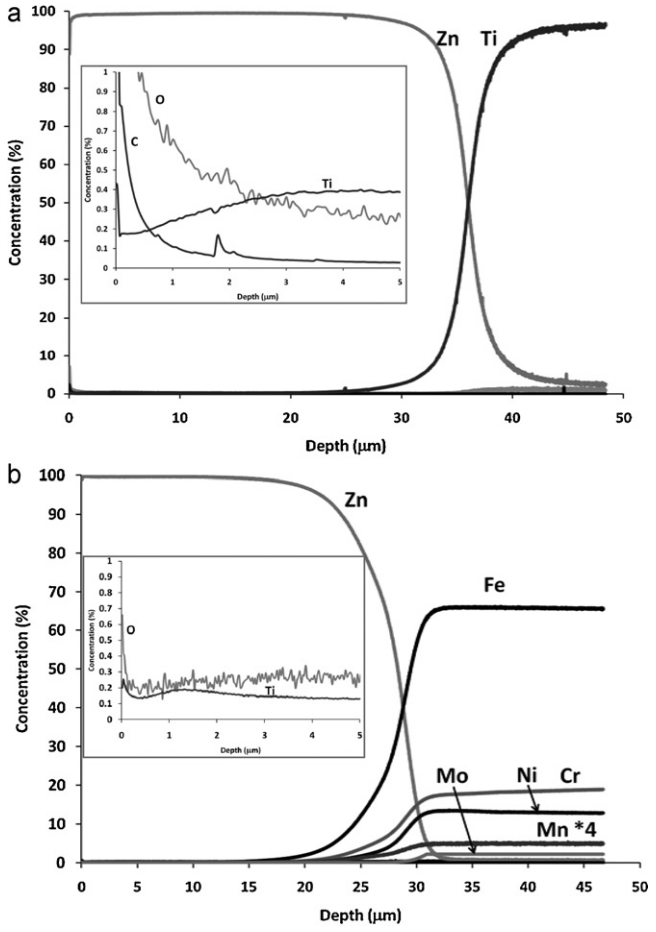

Fig. 5. Quantitative depth profiles obtained by pulsed rf-GD-OES: (a) Zn–TiO_2 nanocomposite film deposited on Ti and (b) Zn–TiO_2 nanocomposite film deposited on steel.

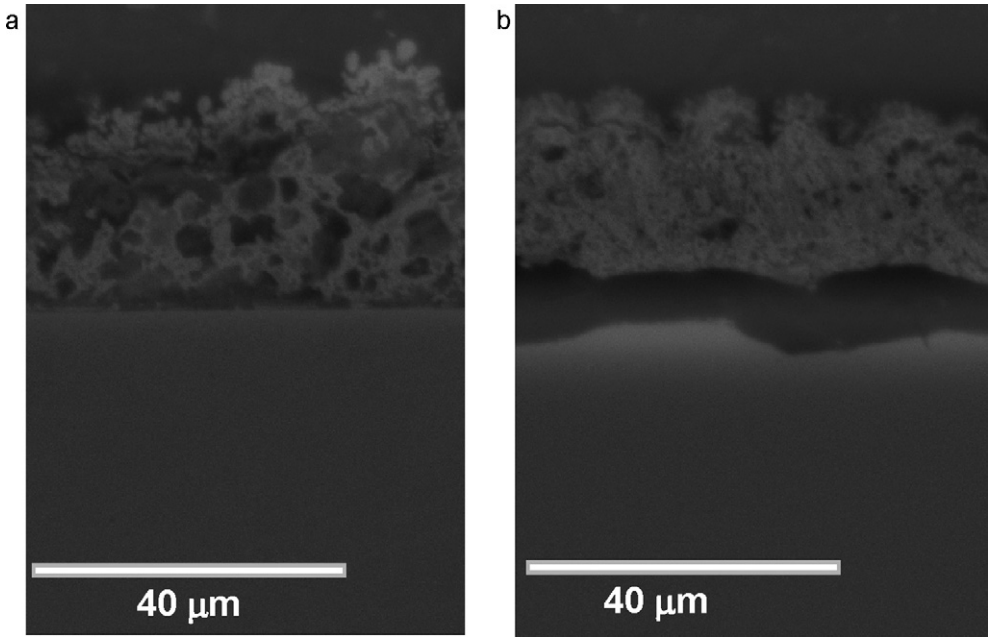

Fig. 6. SEM cross-sections images of Zn–TiO_2 nanocomposite films prepared by pulsed electrolysis. The layers thicknesses measured by SEM are indicated in both cases (standard deviation values are calculated from the mean of measurements in three independent samples): (a) deposited on a Ti substrate (film thickness of 29 ± 4 μm) and (b) deposited on a steel substrate (film thickness of 23 ± 3 μm).

As can be observed in Fig. 5a, a significantly high C and O signals were observed at the beginning of the analysis (first second), which could be attributed to possible contaminations from the sample and anode surfaces and not to the inhomogeneity of the coating; Ti and O profiles showed very stable signals throughout the coating (from 3 μm to the sample interface). Therefore, it could be concluded that the TiO_2 nanoparticles were homogeneously occluded inside the Zn coating.

Concerning the thickness of the nanocomposite films as well as the concentration of the different elements, values obtained by pulsed rf-GD-OES from quantitative depth profiles were validated by comparison with those obtained by SEM and ICP-MS. As can be observed in Fig. 5, the thickness of the Zn–TiO_2 nanocomposite films was found to be around 35 μm (35 ± 2.1 μm) and 28 μm (28 ± 1.6 μm) for the Ti and steel substrates, respectively. These values are well in agreement, within the given uncertainties, with the values obtained by SEM measurements (see Fig. 6). Additionally, Ti concentrations obtained by rf-GD-OES were compared with the values obtained by ICP-MS analysis. From Fig. 5a and b, a Ti concentration in the range of $0.2 \pm 0.021\%$ to $0.4 \pm 0.032\%$ was found in both cases, being this value in good agreement with that obtained by wet chemical analysis using ICP-MS ($0.35 \pm 0.08\%$). Therefore, it seems clear that pulsed rf-GD-OES offers a favorable alternative of accurate and precise depth profiling analysis of Zn–TiO_2 nanocomposite films deposited on different substrates.

In the case of Zn–TiO_2 coatings deposited on Ti substrates, it could be difficult to distinguish between the Ti signal coming from the nanoparticles and the sample substrate due to such element is present at a higher concentration in the substrate than in the coating. However, as has been previously reported for the analysis of Fe in ZnFe-based metallic coatings by ISO standard 16962 [29], the total Ti coating mass per unit area can be calculated taking into account the sputtering time, t_t, when Ti from the substrate begins to appear (time at which the ordinate value for the major element in the coating, Zn, falls to 95% of its maximum or plateau-edge value) and defining the transition zone (between t_t and the time when the Zn profile falls below the detection limit for Zn). Moreover, it should be stated that although the roughness of the Ti substrate can be critical for depth profiling analysis, the crater profiles obtained at the selected experimental conditions showed crater shapes with perpendicular walls and flat crater bottoms.

4. Conclusions

This work demonstrates that pulsed rf-GD-OES is a highly valuable analytical technique for fast and sensitive depth profiling characterization of Zn–TiO_2 nanocomposites, offering a promising analytical tool to assist the synthesis and quality control procedures of nanocomposite's fabrication. Selected experimental conditions in GD pulsed mode allowed good depth resolution for the analysis of Zn–TiO_2 nanocomposite films deposited on conductive substrates. Also, the rf-pulsed mode's advantages (in comparison with the GD continuous counterpart) in terms of emission intensity and emission yields have been demonstrated.

Moreover, the inherent low matrix effects of the GD technique allowed its application, in a multi-matrix calibration procedure, to obtain the quantitative depth profile of the studied nanocomposite films. This is an important capability as the need of resorting to matrix-matched standards is avoided. Therefore, the application of rf-GD-OES in the quantitative analysis of such technological materials, for which reliable matrix-matched standards are not available, is possible. The good results obtained here warrant further work and experiments addressed to investigate this technique performance in other types of nanocomposite films (e.g. Al_2O_3, TaON-Ag).

Acknowledgements

Financial support from "Plan Nacional de I+D+I" (Spanish Ministry of Science and Innovation or MICINN, and FEDER Programme) through the project MAT2010-20921-C02-01 and PT2009-0167, from the EU through the Marie Curie Research Training Network [30] (MRTN-CT-2006-035459) and from the Portuguese Ministry of Science, Technology and Higher Education through Projects PTDC/CTM/64856/2006 and E-33/10 are gratefully acknowledged. B. Fernández acknowledges financial support from

"Juan de la Cierva" MICINN Research Program. Finally, the authors thank ITMA Foundation for technical support with SEM/EDS measurements.

References

[1] B. Fernandez, J.M. Costa, R. Pereiro, A. Sanz-Medel, Anal. Bioanal. Chem. 396 (2010) 15–29.
[2] J.H. Hsieh, C.C. Chang, Y.K. Chang, Thin Solid Films 518 (2010) 7263–7266.
[3] M.E.A. Warwick, C.W. Dunnill, R. Binions, Chem. Vap. Deposition 16 (2010) 7–9.
[4] J.M. Yeh, K.C. Chang, J. Ind. Eng. Chem. 14 (2008) 275–291.
[5] K. Kondo, A. Ohgishi, Z. Tanaka, J. Electochem. Soc. 147 (2000) 2611–2613.
[6] T. Deguchi, K. Imai, H. Matsui, M. Iwasaki, H. Tada, S. Ito, J. Mater. Sci. 36 (2001) 4723–4729.
[7] M. Tavoosi, F. Karimzadeh, M.H. Enayati, A. Heidarpour, J. Alloys Compd. 475 (2009) 198–201.
[8] A.A. Omar, A. Kandil, Metallurgy 60 (2006) 466–470.
[9] Z. Zhan, Y. He, L. Wang, D. Wang, W. Gao, Mater. Process. 24 (2005) 205–211.
[10] A. Fujishima, T.N. Rao, D.A. Tryk, J. Photochem. Photobiol. C 1 (2000) 1–21.
[11] R.E. Steiner, C.M. Barshick, A. Bogaerts, Encyclopedia of Analytical Chemistry, John Wiley & Sons Ltd, 2009.
[12] R. Escobar Galindo, R. Gago, E. Forniés, A. Muñoz-Martín, A. Climent Font, J.M. Albella, Spectrochim. Acta B 61 (2006) 545–553.
[13] R. Matschat, J. Hinrichs, H. Kipphardt, Anal. Bioanal. Chem. 386 (2006) 125–141.
[14] W.W. Harrison, C. Yang, E. Oxley, Anal. Chem. 73 (2001) 480A–487A.
[15] Th. Nelis, M. Aeberhard, M. Hohl, L. Rohr, J. Michler, J. Anal. At. Spectrom. 21 (2006) 112–125.
[16] P. Sanchez, B. Fernandez, A. Menendez, R. Pereiro, A. Sanz-Medel, J. Anal. At. Spectrom. 25 (2010) 370–377.
[17] V. Majidi, M. Moser, C. Lewis, W. Hang, F.L. King, J. Anal. At. Spectrom. 15 (2000) 19–25.
[18] A. Solà-Vázquez, A. Martín, J.M. Costa-Fernández, R. Pererio, A. Sanz-Medel, Anal. Chem. 81 (2009) 2591–2599.
[19] Ph. Belenguer, M. Ganciu, Ph. Guillot, Th. Nelis, Spectrochim. Acta B 64 (2009) 623–641.
[20] M.S. Chandrasekar, M. Pushpavanam, Electrochim. Acta 53 (2008) 3313–3322.
[21] A. Gomes, M.I. da Silva Pereira, M.H. Mendonça, F.M. Costa, J. Solid State Electrochem. 9 (2005) 190–196.
[22] T. Deguchi, K. Imai, M. Iwasaki, H. Tada, S. Ito, J. Electrochem. Soc. 147 (2000) 2263–2267.
[23] B. Fernández, N. Bordel, R. Pereiro, A. Sanz-Medel, J. Anal. At. Spectrom. 20 (2005) 462–466.
[24] B. Fernández, N. Bordel, R. Pereiro, A. Sanz-Medel, Anal. Chem. 76 (2004) 1039–1044.
[25] R.K. Marcus, J.A.C. Broekaert, Glow Discharge Plasmas in Analytical Spectroscopy, John Wiley & Sons Ltd., Chichester, 2003.
[26] D. Alberts, B. Fernández, R. Pereiro, A. Sans-Medel, J. Anal. At. Spectrom. (2011) DOI: 10.1039/c0ja00094a.
[27] V. Hoffmann, R. Dorka, L. Wilken, V.D. Hodoroaba, K. Wetzig, Surf. Interface Anal. 35 (2003) 575–582.
[28] D. Alberts, P. Horvath, Th. Nelis, R. Pereiro, N. Bordel, J. Michler, A. Sanz-Medel, Spectrochim. Acta B 65 (2010) 533–541.
[29] Surface Chemical Analysis—Analysis of Zinc-and/or Aluminum-based Metallic Coatings by Glow-discharge Optical-emission Spectrometry, ISO 16962: 2005.
[30] http://www.gladnet.eu.